

THE SETHI REMOTE SENSING AIRBORNE PLATFORM AND THE RELATED SCIENCE ACTIVITIES

Pascale Dubois-Fernandez¹, Olivier Ruault du Plessis¹, Aurélien Arnaubec^{1,2}, Sébastien Angelliaume¹, Remi Baqué¹, Grégory Bonin¹, Xavier Briottet¹, Hubert Cantalloube¹, Patrick Chervet¹, Colette Coulombeix¹, Philippe Deliot¹, Philippe Dreuillet¹, Xavier Dupuis¹, Philippe Durand³, Delphine Fontanaz³, Patrick Fromage¹, Daniel Heuzé¹, Philippe Martineau¹, Hélène Oriot¹, Philippe Paillou⁴, Thuy Le Toan⁵, Bernard Vaizan¹

1: ONERA, the French Aerospace Lab, Salon de Provence, Palaiseau, Toulouse – FRANCE

2: Institut Fresnel, CNRS, Aix-Marseille Université, Marseille – FRANCE

3: CNES, the French Space Agency, Toulouse – FRANCE

4: OASU – Université Bordeaux 1, Bordeaux – FRANCE

5: CESBIO - Université Paul Sabatier, Toulouse – FRANCE

Résumé

L'ONERA, le laboratoire français en aérospatial, construit des systèmes radar aéroporté depuis plus de deux décennies pour des applications de défense mais aussi scientifiques. Au cours des six dernières années, l'instrument SETHI, embarqué à bord d'un avion Falcon 20, a été développé principalement pour des applications scientifiques. Dans cet article, la philosophie de son développement est mise en exergue et les instruments sont décrits en détails. L'instrument SETHI comprend trois systèmes radar en bandes P, L et X, une caméra dans le domaine visible, en visée oblique afin de suivre le champ de vue des radar, et une caméra hyperspectrale à visée au nadir. Cet article résume alors les dernières campagnes SETHI dans le cas de préparation de deux missions spatiales. Il s'agit tout d'abord de la mission de l'ESA, BIOMASS, comprenant un radar bande P pour la cartographie de la biomasse à grande échelle. La deuxième mission traite de surveillance maritime et comprend un radar en bande X. Pour chaque campagne, les principaux objectifs sont détaillés, les références aux articles correspondants sont fournies et les principaux résultats sont mis en avant. Finalement, l'article fournit un aperçu des prochains développements liés au système SETHI dans le cadre de la fusion de données optique et radar.

Mots clés : RSO, optique, hyperspectral, biomasse, surveillance, fusion.

Abstract

ONERA, the French Aerospace Lab, has been designing airborne radar for more than two decades for Defence oriented applications, as well as for science applications. In the past six years, the SETHI instrument, hosted on board a Falcon 20 aircraft, has been developed with a main focus on science applications. In this paper, the philosophy of this development is highlighted together with a detailed description of the instruments. The SETHI instrument includes three SAR systems at P, L and X bands, one context camera in the visible domain, with a side looking geometry matching the radar field of view, and a hyperspectral camera with standard nadir geometry. The paper then summarises the latest SETHI campaigns in the context of two spaceborne mission preparations. The first is the ESA BIOMASS mission with a P-Band SAR instrument for global forest biomass mapping. The second one is a maritime surveillance mission, including an X-band SAR system. For each campaign, the main objectives are listed, the references to the dedicated papers are provided and the major results are highlighted. Finally the paper then provides a preview for the future developments around the SETHI system, for studies dedicated to the optical/radar data fusion.

Keywords : SAR, optical, hyperspectral, biomass, surveillance, fusion.

1. Introduction

With many spaceborne Earth observation missions already in operation, the role of airborne sensors has naturally evolved to fill the gaps not covered by space instruments.

In particular, airborne remote sensing is an essential tool for the preparation of future space missions. It can

provide essential test datasets, not yet available from space. These airborne datasets are important at every stages of the mission design cycle. In the feasibility phase, they demonstrate an observation technique. A little further in the design cycle, they contribute to specifying the system parameters required to meet the desired science objectives. Later in the process, they trigger methodological developments for the definition of

the spaceborne mission ground segment, and allow the definition of the future retrieval algorithms by providing a basis for bench marking and evaluation. Finally they are an important aspect of the calibration/validation phases. In parallel, and in a complementary manner, the airborne solution enables resolution and flexibility that are not yet accessible from space. Beyond the more precise vision associated intrinsically with the airborne campaigns, high resolution imagery is a key element in the multi-scale approach required to globally understand our environment.

Another unique characteristic of airborne imagery, compared to its spaceborne counterpart, is its unconstrained revisit time. Indeed, airborne observation can be repeated on request several times a day, or at specific times. It thus opens the way to the study of the circadian cycle or alternatively, and contributes to the selection of the best time of observation, e.g. in the case of a future sun-synchronous satellite.

As a summary, the airborne solution offers a large range of observation characteristics that are not possible from space (e.g. spatial resolution, observation geometry, spectral or frequency band, revisit rate).

Several research organizations own airborne SAR systems, for example DLR (Germany) (Horn, 1996; F-SAR, 2012), INDRA (Spain), NASA (USA) (Rosen et al., 2006), etc. The ONERA SETHI system stands out compared with these other systems on three main aspects:

- Its capacity to simultaneously integrate a wide variety of optical and radar instruments;
- The flexibility of the acquisition geometry for each of the sensors characterized by adjustable acquisition configurations;
- The very high achievable spatial resolution of the radar instruments.

In this paper, we describe the SETHI system and illustrates how in the last four years, several data acquisition campaigns were conducted in order to support the design of future satellite missions. Two specific examples are presented: the BIOMASS mission (Le Toan et al., 2011) and a sea surveillance mission (Richard et al., 2010). These two projects are at different design stages. The BIOMASS project has been studied since 2007 whereas the sea surveillance mission is in a preliminary feasibility phase.

Another facet of our research implication is the study of the radar/optical data fusion for science applications. To this effect, a dedicated ONERA project, relying on the in-house optical and radar expertise, explores the synergy between radar and optical data for vegetation characterisation and land use/ land cover mapping. This project relies on acquisitions conducted simultaneously with P-band and L-band SAR and visible and near-infrared (VNIR) hyperspectral imagery.

2. The SETHI system

2.1. Description

The SETHI airborne imaging radar project was initiated in 2005 as a successor of RAMSES (Dreuillet et al., 2006), ONERA previous airborne radar platform. RAMSES was hosted on board a Transall which was decommissioned in 2008. SETHI (Baque et al., 2009), on board a Falcon 20 operated by the AVDef company, is mainly dedicated to science applications. It combines two under-wing pods (Figure 1), and five electronic bays located inside the cabin. The pod-based concept was chosen to facilitate the upgrade of existing radars and the integration of new radars. Once the flight certification is obtained for a generic configuration, both the cabin bays and the pod equipment can be modified within certain limits without triggering another cumbersome certification phase. The pods can accommodate different radar sensor payloads ranging from P-band to Ku-band and/or optical sensors. In this first implementation, the radar instruments are at P-band, L-Band and X-Band.



Figure 1 : The Falcon 20 after take off and under-wing pods.

The pod outer envelope is transparent to electromagnetic waves in a large range of frequencies (from 200 MHz to 18 GHz) and the main support beam guarantees the integrity and safety of the installation. The useful length of each pod is 2.3 m, the diameter is 0.535 m and the payload maximum weight is 120 kg per pod. An optical window in the nose of the pods can accommodate an optical instrument (Figure 1).

The low frequency radar system is referred to as P-Band but in reality it covers a larger spectrum from 220 MHz to 460 MHz (very high frequencies (VHF) → ultra high frequencies (UHF)).

Table I summarizes the characteristics of SETHI radars.

| Radar | P | L | X |
|--|-------------------------|-----------------------------------|----------------------|
| Center frequency (MHz) | 340 | 1300 | 9500 |
| Instrumented bandwidth (MHz) | 240 | 200 | 1500 |
| Best achievable resolution (cm) | 62 | 75 | 10 |
| Polarisation | Full | Full | Full |
| Transmit peak power (W) | 500 | 200 | 200 |
| Antenna | Dipoles | Patch array | Horns |
| Elevation aperture (°) | 100 | 30 | 14 |
| Azimuth aperture (°) | 50 | 10 | 14 |
| Boresight incidence | -65° to 0° Left look | -65° to 85° Left or right look | 0°-90° Right look |
| Number of required channels for polarimetric mode | 1 | 2 | 2 |
| Number of available recording channels | 4 | | |
| Maximum sampling frequency (GHz) | 2 | | |
| ADC bandwidth (GHz) | 3 | | |
| ADC dynamic (bits) | 10 | | |
| Data rate/channel (MB/s) | 360 | | |
| Record capacity (TB) | 1.6 | | |

Table 1 : SETHI characteristics.



Figure 2 : X-Band SAR image of the Viaduc de Millau (*Millau bridge*), France.

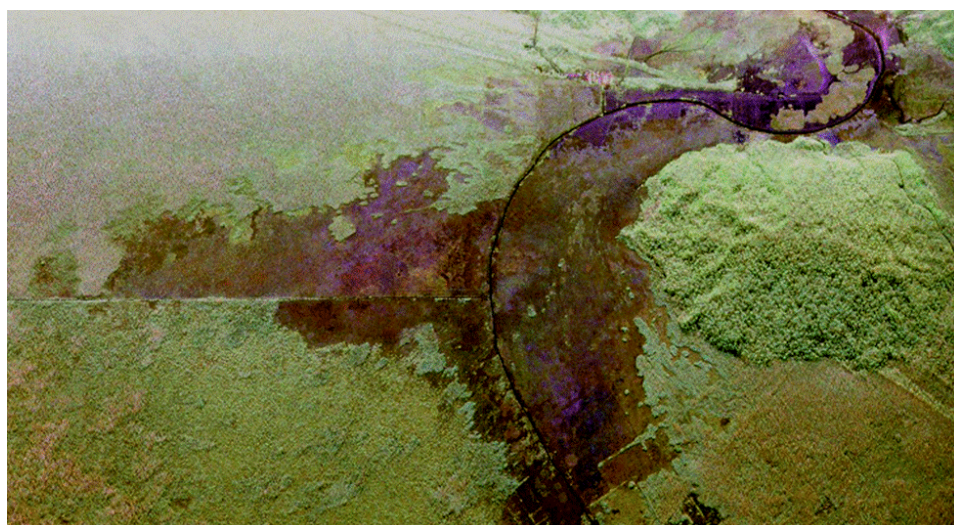


Figure 3 : The Marais de Kaw (*Kaw marsh*) in French Guiana acquired during the TropiSAR campaign at P-Band.

The P-Band antenna is located in the left pod (left looking geometry only) while the L-band and X-band antennas are in the right pod (see Figure 4). The L band antenna can be right or left looking, with incidence angle in the range of -65° to 85° . The X band horns are right looking and can be oriented from Nadir to 90° . All radars are fully polarimetric.

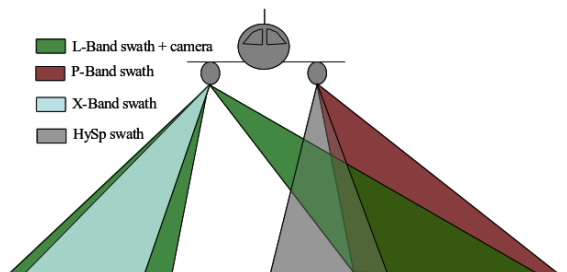


Figure 4 : The different observation geometries associated with the SETHI payloads.

They can be operated with the full bandwidth or with a waveform adapted to match a given centre frequency (in the instrumented range), bandwidth (which translates into resolution), mode of acquisition (single polarisation, dual polarisation or full polarisation), and boresight angle. All these modifications in the acquisition configuration can be performed while the system is airborne, allowing a variety of operating modes during a single flight. Compared to the other airborne SARs available in the community, SETHI has a unique versatility, being able to provide simultaneous acquisitions at P and L or at L and X-band, associated with a flexible geometry. The flight altitude is limited to 30000ft above Mean Sea Level. When two radars are operated simultaneously, the system relies on an external auxiliary power unit, for which the flight altitude is limited to 13000 ft. In the following paragraph, we will see how the waveform can be adapted according to specific objectives.

The SAR processing is performed with the Pamela software (Cantalloube and Dubois-Fernandez, 2006; Cantalloube et al., 2010) developed and operated by the SETHI team. In Figure 2, an example of an X-band high resolution acquisition over the Millau bridge is presented. The shadows of the different parts of the bridge are clearly visible. The post-processing of the SAR data includes a calibration step for which some specific targets are deployed across the swath of the calibration site. The calibration technique is following the Sarabandi method (Sarabandi et al., 1990). Usually the calibration set up includes between two and five trihedrals with a size large enough to create a backscatter of at least 25dBm^2 , and a dihedral oriented at 22.5° providing an equivalent radiometric response in the four polarisation channels (HH, HV, VH and VV). Typical sizes for the reflectors, as a function of frequency, are given in Table 2.

In the following sections, we will describe how the latest SETHI campaigns dedicated to science applications were designed in order to provide inputs to space mis-

| | UHF Band | L-Band | X-Band | | |
|--|----------|--------|--------|------|------|
| Trihedral size (m) | 2.275 | 1.77 | 0.97 | 0.70 | 0.56 |
| Radar Cross-section (dBm^2) | 23.7 | 28.2 | 35.6 | 30.0 | 26.1 |

Table 2 : Size of the trihedral corner reflectors used for the system calibration.

sion projects such as BIOMASS and a maritime surveillance mission.

3. Activities in the context of the BIOMASS mission TropiSAR

BIOMASS meets a pressing need for global information on carbon sinks and sources in the forests, which is of essential value for climate modelling and policy adaptation, e.g. REDD (the United Nations Collaborative Programme on Reducing Emissions from Deforestation and Forest Degradation in Developing Countries).

Knowledge about forest above-ground biomass is of fundamental importance in quantifying terrestrial carbon sinks and sources, required for climate change understanding. In many parts of the world, in particular the tropical forests, information on biomass is currently very limited and subject to large and unquantified errors.

In response to the urgent need for improved global biomass mapping and the lack of current space systems capable of addressing this need, the BIOMASS mission was proposed to the European Space Agency (ESA) for the third cycle of Earth Explorer Core missions. It is at present time the Core Earth Explorer candidate mission currently investigated by ESA (European Space Agency, 2008; Le Toan et al., 2011). BIOMASS is a P-Band SAR mission, intended to provide first observations of the global distribution of forest biomass, and to monitor the biomass changes throughout the mission duration. BIOMASS would be the first P-Band SAR in space, opening the way to many secondary applications, such as subsurface feature cartography in arid environment or topography mapping under dense forests. BIOMASS would be the first P-Band SAR in space, opening the way to many secondary applications, such as the cartography of subsurface features in arid environment.

SETHI has been commissioned to support the preparation phase of the BIOMASS mission. Three campaigns have been conducted to that purpose: TropiSAR over a tropical forest, BioSAR2010 over a Boreal forest and TuniSAR over a semi-arid region.

- TropiSAR (Dubois-Fernandez et al., 2008) was conducted in August 2009 in French Guiana to validate and refine the algorithms developed over Boreal and Temperate forests for dense forests.

- BioSAR2010 (Ulander et al., 2011) was designed as a complement to a previous campaign conducted in 2007 by DLR E-SAR over a forest site in Sweden. The main purpose was to explore the change in forest cover and forest biomass after a three-year period.
- TuniSAR (Paillou et al., 2010) was flown in 2010 in South Tunisia in order to explore the potential of a P-Band radar for the cartography of arid areas.

3.1. TropiSAR

The campaign consortium included ONERA, CES-BIO (Center for the Study of the Biosphere from Space), CIRAD (Center of Agricultural Research for Development), and EDB (Evolution and Biological Diversity) lab of the University of Toulouse. The project was financed by ESA, CNES and ONERA. A detailed description of the TropiSAR campaign can be found in (Dubois-Fernandez et al., 2008). In this paper, we provide an overview of the campaign objectives and the main results.

The two main studied sites, Nouragues and Paracou were selected to be representative of the dense tropical forest in South America. Both sites are existing research sites, established in the 80's that have been extensively monitored for more than two decades. The forest sites where in-situ data are available cover more than 150 ha, with more than 98000 trees which have been marked, identified and measured. The SAR acquisition geometry was defined to provide an incidence range including the steep configuration. It is foreseen in the BIOMASS mission with a near range incidence angle of approximately 25° - 30° . The airborne platform was flown close to the flight ceiling of SETHI when operating two radars simultaneously, which is 13000 ft. It was decided to acquire simultaneously P and L band polarimetric images in order to compare the performances of P-band and L-band for BIOMASS retrieval. The waveform (transmit bandwidth, flight altitude, ...) can be adjusted on SETHI and was specifically optimised for this mission. 37 radar images have been processed at P-Band and L-Band (see Figure 2). The TropiSAR dataset is made available to interested scientists via the campaign data archive of the European Space Agency (ESA).

Details on access to campaign data can be found at the ESA EOPI portal (<http://eopi.esa.int>) under the campaigns link.

In this paper dedicated to the SETHI system, we choose to highlight two main results from the TropiSAR campaign: the temporal stability of the backscattering signature over the 23 day period, both in backscatter intensity (radiometry) and in interferometric coherence, and the great capacity of the P-Band PolInSAR technique to characterize the under-canopy topography. For more details about the campaign results, the reader can refer to the TropiSAR dedicated paper (Dubois-Fernandez et al., 2008).

Previous studies have shown that the P-band SAR intensity of the cross-polarised signal (HV) can be related to the values of above ground biomass (Le Toan et al., 1992; Rignot et al., 1995; Saatchi et al., 2007; Hoekman and Varekamp, 2008; Sandberg et al., 2011). However, the relationship could be affected by changes in the environment (winter/ summer conditions, soil and vegetation moisture...). This was observed over Temperate and Boreal forests. The temporal behaviour of P-Band backscatter over tropical forests had not been studied and this was one of the main objectives of the TropiSAR campaign.

To quantify the temporal variation of the backscattered intensity, the backscatter coefficients of the reference forest plots have been analysed for each of the seven acquisition dates during the 23 days of the campaign. The reference plots are 16 square forest plots in Paracou (15 plots of 250 m x 250 m and one plot of 500 m x 500 m) characterized by different forestry treatments. The plots have sufficient size (250m x 250m at Paracou) to reduce change in the backscatter due to speckle and location error effects. The stability of the HV backscatter response observed during the 23 day period of the TropiSAR campaign is excellent with an observed variation of less than 0.5dB, which is the order of the instrument radiometric accuracy (see Figure 5). This is an important observation as it indicates a certain robustness of the radiometric inversion with respect to temporal variation linked to local conditions.

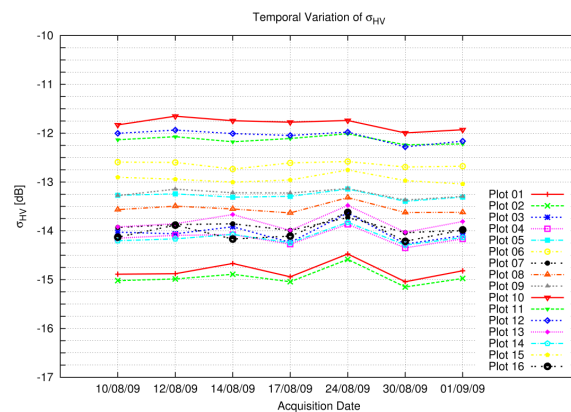


Figure 5 : Variation of the backscattering coefficient σ_{HV} for the 16 plots over the Paracou test sites during the 23 days of the campaign.

The polarimetric Interferometric SAR technique (PolInSAR) is based on the combined analysis of two complex polarimetric SAR datasets acquired in slightly different geometries. Polarimetry allows the exploration of the different scattering mechanisms involved in the wave/vegetation interaction while interferometry provides information about the elevation of the corresponding scattering centers. This height variation with polarisation can be used to characterize the forest structure. One well-known model is the Random Volume Over Ground

model (RVoG) (Cloude and Papathanassiou, 2003). For the spaceborne BIOMASS mission, the two datasets with different geometries can only be acquired in a repeat path mode in the case of BIOMASS with one orbit cycle delay between the two acquisitions. Interferometry requires that both acquisitions stay coherent over this period.

In past airborne studies over tropical forests, the temporal delay of the repeat pass acquisitions was less than one day. One of the objectives of the TropiSAR campaign was to assess whether the interferometric coherence would remain high for images acquired in successive orbit cycles, 20 days or so apart over tropical forests. The TropiSAR data analysis showed that the coherence indeed remains high even after 23 days (see Figure 6) with a slightly higher observed coherence at HH than at VV or HV.

This result indicates that over tropical forest, the repeat pass mode can provide PolInSAR datasets suitable for vegetation characterisation.

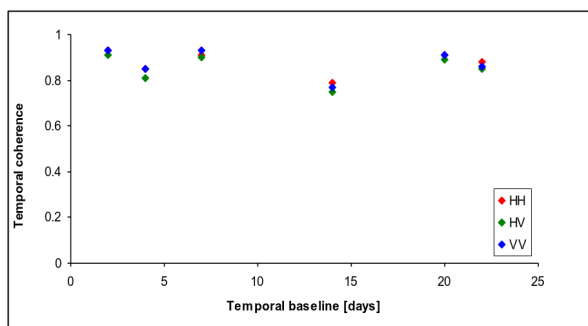


Figure 6 : Interferometric coherence as a function of temporal baseline for the three linear polarisations HH, HV and VV.

The PolInSAR technique can also provide estimates of the under-canopy ground height. In Figure 7, the estimated ground height is compared to the LIDAR derived ground height (Lidar data courtesy of CIRAD) and shows a very good agreement with a RMS difference less than 3 m (Arnaubec et al., 2012). The forest is dense, with biomass from 250 to 450 ton/ha and tree height ranging between 30 m and 50 m.

The dataset is still being analysed by several research teams in France and in the international community. More results are expected to be published in the near future. In particular, it was found that the full biomass range in French Guiana can be estimated using the P-band SAR data, with an increased accuracy when the SAR intensity is used jointly with PolInSAR and tomographic techniques (European Space Agency, 2012).

3.2. BioSAR2010

BioSAR 2010 (BioSAR-3) (Ulander et al., 2011) is the most recent data collection experiment undertaken within the BIOMASS framework and funded by ESA. The consortium included FOI, SLU, Chalmers University

from Sweden, and ONERA. The first two eponym campaigns, BioSAR 2007 (BioSAR-1) (Hajnsek et al., 2008) and BioSAR 2008 (BioSAR-2) were carried out already during the Assessment Study with the DLR's airborne SAR E-SAR and took place in Sweden, at test sites consisting of hemiboreal forest types.

The BioSAR 2010 campaign was defined to address additional requirements linked to the BIOMASS mission. In particular, the campaign explores the ability of the mission to detect and map temporal changes in forest biomass and disturbances. These represent an intrinsic element of the mission concept and exploitation but for which suitable data sets are lacking. So as to be able to study the changes of forest conditions the test site is the same as in BioSAR 2007, i.e. Remningstorp in Southern Sweden. The SAR sensor used for this new experiment was SETHI. The inherent flexibility of SETHI could be used to match the geometric configuration of the previous E-SAR acquisition.

It was found that major changes such as clear-cutting and thinning were readily visible on the SAR images. Furthermore, the interferometric coherence was found to stay high over some stands even after a three years period.

This is illustrated Figure 8 with the SETHI P-Band image acquired in October 2010, the E-SAR P-Band image over the same zone acquired in April 2007 and the interferometric coherence between the two datasets for the HH polarisation. Processing the SETHI data in order to match the geometry of the two SAR systems was tricky and a full description of the process is provided in (Dupuis et al., 2012).

3.3. TunisSAR

Access to freshwater resources is a crucial point for future generations, in particular in semi-arid and arid regions such as North Africa. Currently, typical water prospecting schemes initiate from existing geological maps, from which further fieldwork explorations are defined (geophysical prospecting, drilling). Several pilot projects have shown the usefulness of Earth observation data for water resources prospecting. However, a strong limitation of remote sensing is the fact that most of the relevant geological features in arid regions are hidden under a thin layer of aeolian sandy sediments. Subsurface geology (bedrock of volcanic rocks, limestone and sandstone) is then generally invisible for optical remote sensing instruments.

On the opposite, low frequency radar has the potential to image these structures. As an example, previous observations have demonstrated that at L-band, electromagnetic waves can penetrate about 1.5 m into dry sandy sediments (McCauley et al., 1982; Paillou et al., 2010). For P-band, the penetration depth is expected to be three times greater, that is about 4.5 m. This has been confirmed by aircraft campaigns at P-Band in the United States and in France (Farr, 2001; Paillou and Dreuillet, 2002). Furthermore, a longer wavelength system, such

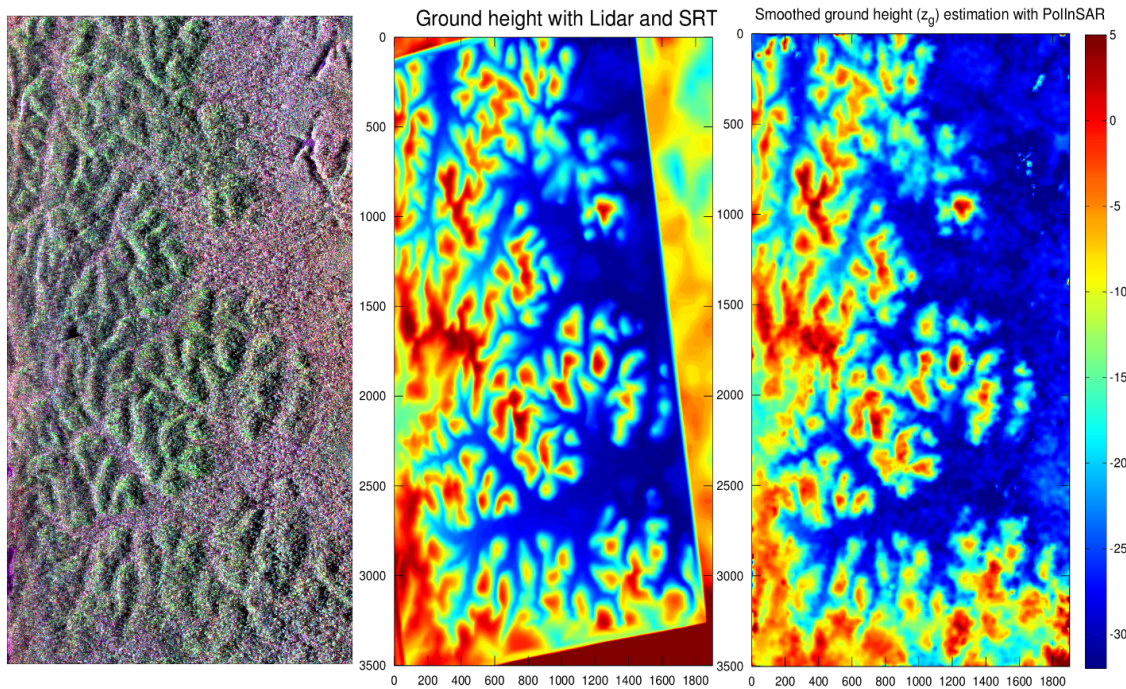


Figure 7 : Backscatter image of the studied site of Paracou with HH in red, HV in green and VV in blue. Lidar ground height in the white box (courtesy of CIRAD) completed with SRTM© height outside the white box in the middle image; PolInSAR ground height in the right image.

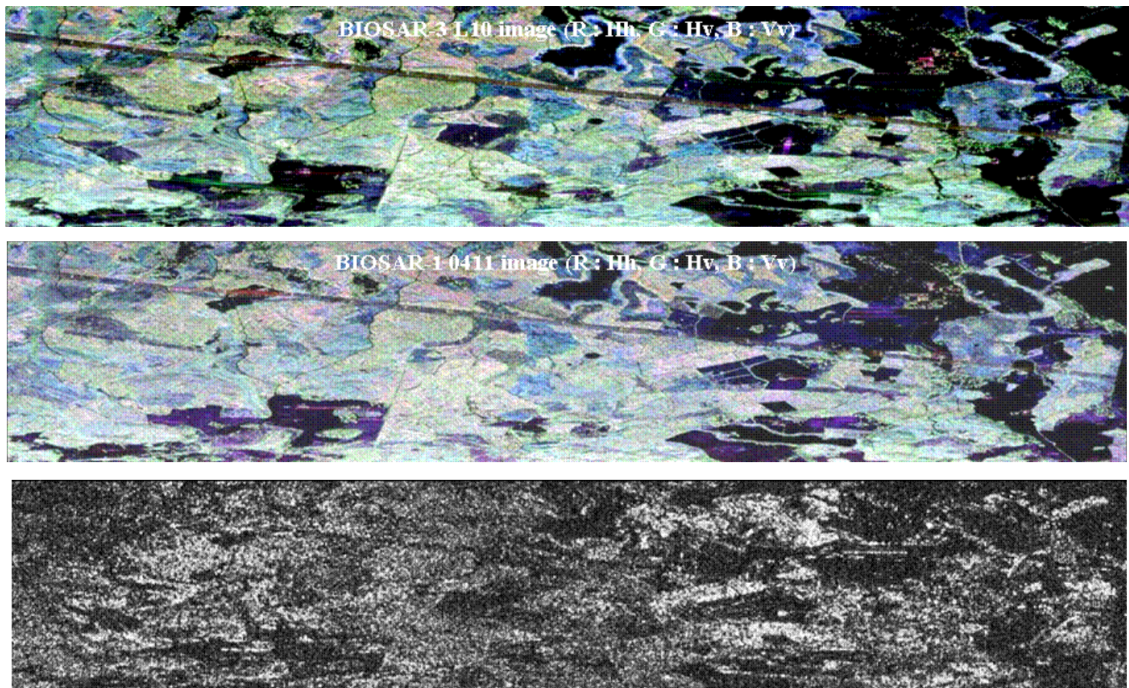


Figure 8 : SETHI P-Band image acquired in October 2010 (top), E-SAR P-Band image (middle) acquired in April 2007 with HH in red, HV in green and VV in blue (Courtesy of DLR), interferometric coherence between the two dates for the HH channel scaled between 0 and 1 (bottom).

as P-band, should also be less sensitive to volume scattering which might occur in the covering sediment layer due to gravels and small rocks. It sometimes screens the sub-surface structures at L-band. Within the framework of a cooperation project between the University of Bordeaux, the ONERA/DEMR, and the Centre National de la Cartographie et de la Télédétection (*Cartographic and Remote Sensing National Center*) de Tunis, with a financial support of the French Space Agency CNES, we conducted an airborne P-band SAR campaign over Southern Tunisia during June 2010. The TunISAR experiment (Paillou et al., 2010) aimed at evaluating potentials of low-frequency SAR for sub-surface geology mapping, and it was the first time a P-band synthetic aperture radar was flown over Sahara. Comparison between TunISAR P-band data and higher frequency L-band PALSAR data allows to quantify the benefits of P-band for mapping sub-surface geology.

We considered some acquisitions performed over the Ksar Ghilane oasis (N32.98 - E009.64), the most Southern oasis in Tunisia. Once again, SETHI flexibility proved to be essential. Indeed, the acquisition characteristics had to be modified while the system was already in Tunisia in order to comply with a last minute notification of the electromagnetic emission restriction over the Tunisian airspace. Full polarimetric data were acquired at a resolution of 3 m, for a central frequency of 435 MHz. Figure 9 shows the Ksar Ghilane oasis region imaged with optical data (source Google Earth) and the corresponding topography (source SRTM). The oasis lies East of an ancient river bed now filled with sand.

To compare L-band and P-band sub-surface imaging performances, we used an ALOS/PALSAR scene of the Ksar Ghilane oasis, with a resolution of 12.5 m at an incidence angle close to 34°. Figure 9 shows also both PALSAR (L-band) and SETHI (P-band) SAR images. The resolution of the SETHI image was reduced to be comparable to the PALSAR one. In the South of the oasis, the differences between both images are clearly visible: P-band allows to clearly map many secondary river tributaries, while L-band only shows one structure. The L-band signal is mainly dominated by the surface scattering of the superficial sediment layer, which hides the sub-surface contribution. On the opposite, at P-band, the superficial layer is smoother and contributes less to the total backscattered power, making the sub-surface contribution more visible. Field work has been conducted in June 2012 in order to map sub-surface channels using geo-radar and thus confirms the penetration depth of the P-band SAR.

4. Activities in the context of sea surveillance

With the increased occurrence of piracy and ship related oil spills, surveillance of oceans and seas is becoming a key issue. SAR systems can provide a significant contribution in detecting cooperative and

non-cooperative ships, consistent with an observation frequency adapted to the needs of maritime surveillance. CNES is studying a mission concept with a SAR system operating at grazing incidence angles in order to meet this objective (Richard et al., 2010; Angelliaume et al., 2011).

In this context, an acquisition campaign involving SETHI, took place over the Atlantic Ocean, off the Brittany Coast of France, in November / December 2011. The aim was to complement existing full-polarimetric SAR databases for various conditions of acquisition and especially at low grazing angle (incidence angle up to 80°) in order to improve the Radar Cross Section and reflectivity knowledge needed for detection performance assessment.

This is yet another example where SETHI flexibility is essential. The system geometry can be modified, even during one flight, allowing different incidence angles from one acquisition to the next. It thus allows to cover the full range of potential geometries (from 50° to 80°) in order to provide consistent sea backscattering coefficient as a function of incidence angle for one particular sea state.

In Figure 10, the potential of X-band imagery at grazing incidence angle and high resolution is highlighted. Figure 11 presents a maritime image over the Palay in Brittany. The wave pattern is clearly visible. A small boat can be seen in the top part of the image with the typical streaking effect.

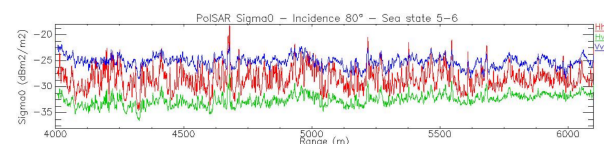


Figure 12 : Sigma0 values at grazing angle for the three linear polarisations for a sea state of 5-6.

In Figure 12, the observed sigma0 values for a sea state of 5-6 are around -25 dB for VV, -28 dB for HH and -32 dB for HV. The VV response presents less variation than the HH response. Looking at the individual images, the HH image appears to be strongly affected by Doppler effects (smearing of the image in the azimuth direction) possibly linked to more local phenomena such as breaking of the waves. The HV measure is certainly affected by the noise floor, estimated to be around -34 dB at near range.

5. Exploring new frontiers

With the expected increased availability of Earth Observing instruments in the next decades, it is important to explore the joint use of datasets from different instruments. Data fusion between optical and radar data, between different radar frequencies, and different optical

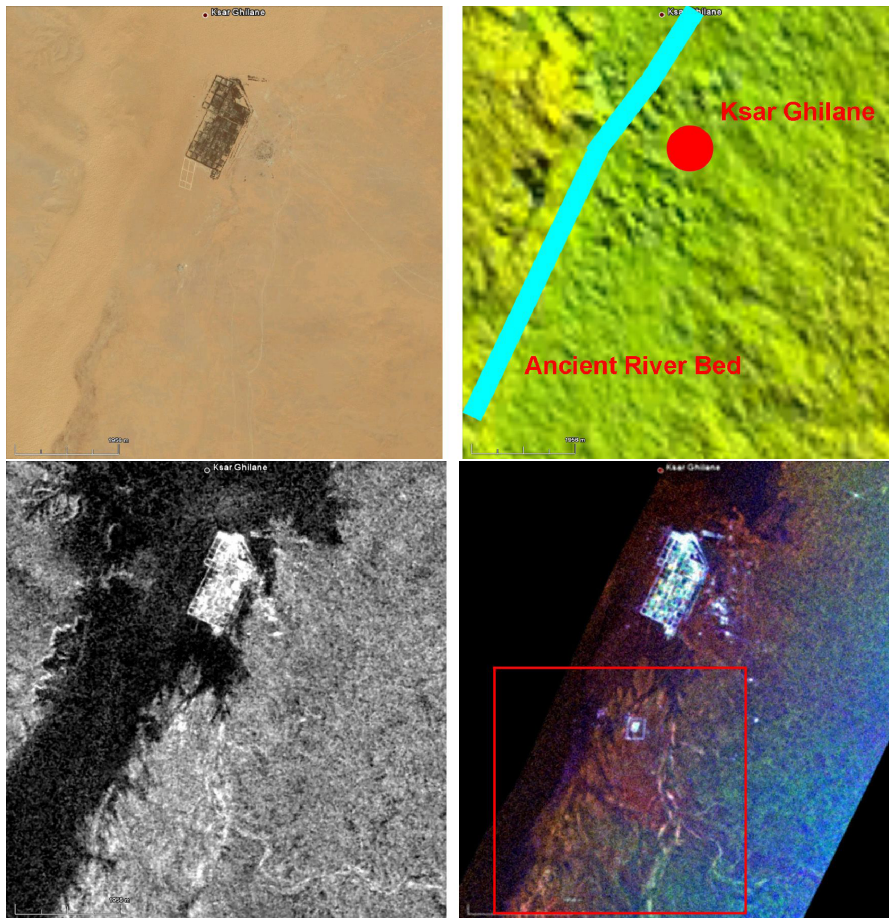


Figure 9 : The Ksar Guillane area in Tunisia; Google Earth image © (top left), SRTM DEM NASA ©(top right), PALSAR JAXA© image (bottom left), SETHI P band SAR image (Red HH, green HV, blue VV) (bottom right) with an equivalent resolution as PALSAR image.



Figure 10 : X-Band Polarimetric image at grazing incidence angle (80°) acquired during the MENAS-BIS campaign.

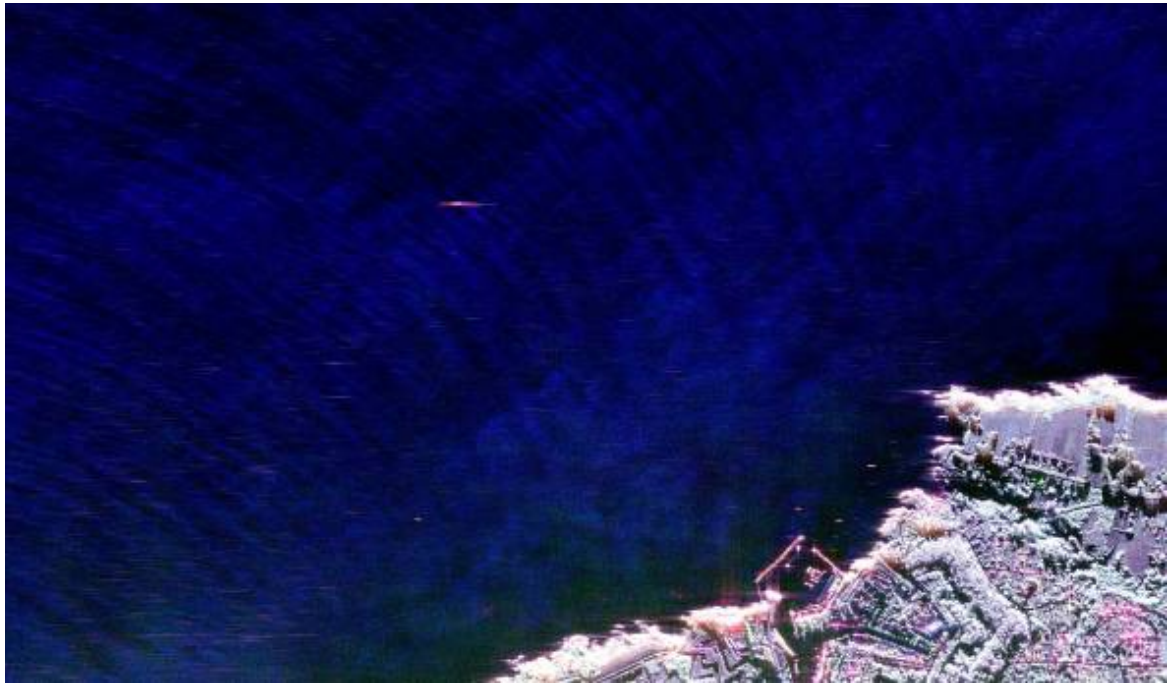


Figure 11 : X-band image acquired with a 70° boresight incidence angle of the coast of Brittany, France. The colors are from polarimetry with HH in red, HV in green and VV in blue. The harbor in the bottom right of the image is le Palais.

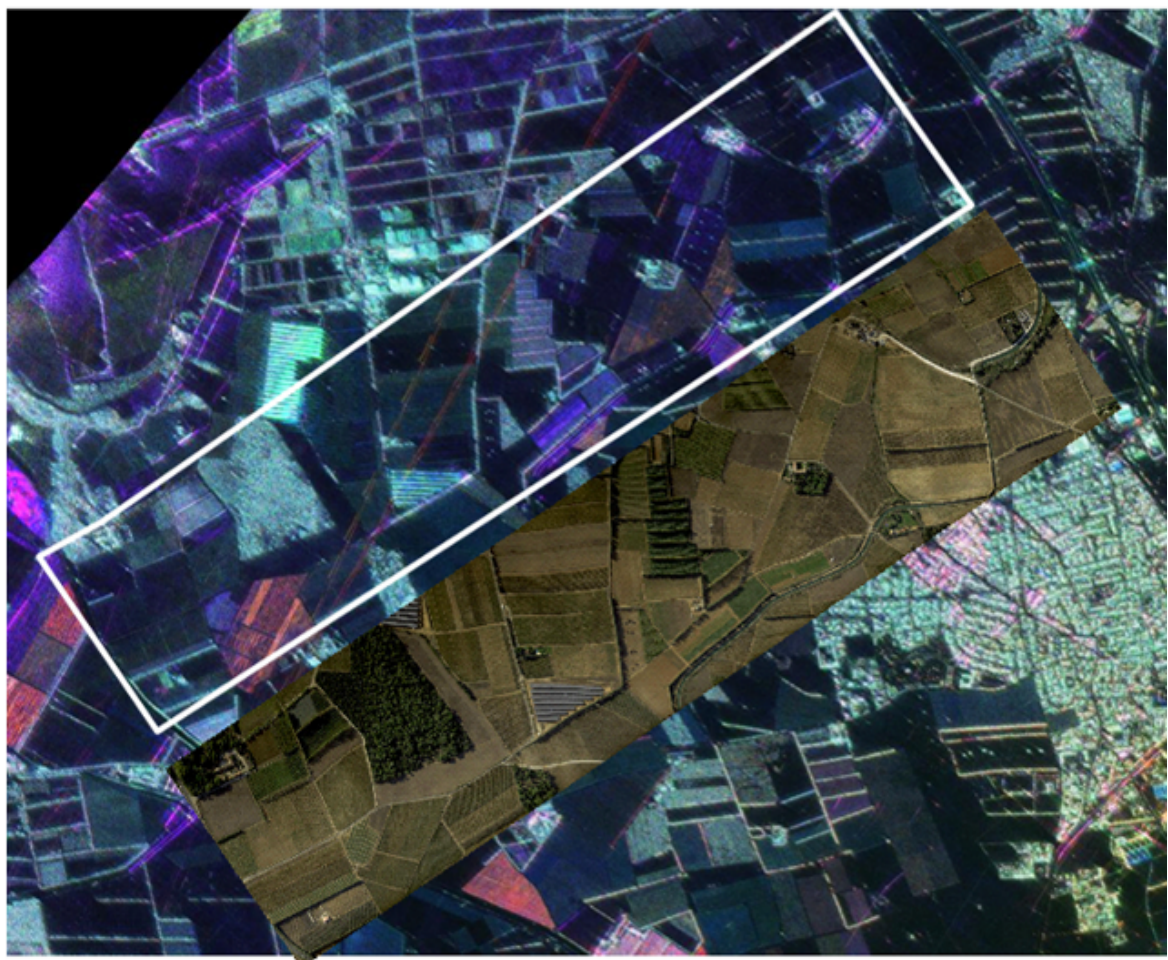


Figure 13 : P-Band image (HH red, HV green, VV blue) with a VNIR hyperspectral image overlaid.

domains is a promising field. SETHI can contribute to this development by providing simultaneously acquired datasets. In October 2011, we conducted an acquisition campaign in Southern France where UHF-Band, L-Band fully polarimetric data as well as HySpex VNIR hyperspectral imagery were acquired at the same time. Evaluation of the potential of data fusion for agricultural crop identification and vegetation characterisation is ongoing at ONERA under internal funding with the ENVIRO project. In Figure 13, both the P-Band SAR image and the VNIR hyperspectral image are presented as an illustration of the combined synergy of the two electromagnetic domains. In this example, the complementarity between optical instrument and P-Band radar can be highlighted in the three areas in the blue, red and green boxes. In the blue box, the radar image identifies poles located regularly in the field hardly visible in the optical imagery without using adapted features. The red lines in the radar images are power lines which stay completely invisible on optical imagery even after processing due to the lack of contrast and resolution. The agricultural field in the green box corresponds to market gardening with different types of vegetables planted in a single field along rows. The radar image discriminates between the different crops, certainly due to the different structures of the plantation, while in the hyperspectral image the signature is dominated by the leaf response and seems uniform. In the red box, the optical image shows variations between the long cultivated strips that are not visible in the radar image.

6. Conclusions and perspectives

In this paper, we have described SETHI, the ONERA airborne experimental platform including three fully polarimetric imaging Synthetic Aperture Radars, one hyperspectral camera, and one visible camera. The originality of the SETHI system lies in three main aspects, making it at the forefront of the technology:

- The potential simultaneity of the acquisitions with different instruments;
- The flexibility of the acquisition characteristics (geometry, waveform, resolution, mode of operation);
- The very high spatial resolution with all the available instruments, in particular in the microwave range.

These three aspects are illustrated through the description of the latest acquisition campaigns performed with SETHI in the framework of sciences applications. Campaigns were conducted in support of two spaceborne mission projects, and in order to investigate the synergy between radar and optical data. The work is still on-going but SETHI is now in operation, producing high quality datasets in a broad electromagnetic spectrum.

Acknowledgements

The studies presented in the paper were conducted under ESA (contract N° 22446/09 No. 4000102509/10), CNES-TOSCA TropiSAR support, TuniSAR support, BIOMASS support CNES N°116238/00, and ONERA (SETHI, PRF ENVIRO, RG-BIOMASS) fundings. The authors want to acknowledge the precious help from L. Ulander, A. Gustavsson, X. Fransson in the BIOSAR campaign, J. Chave, L. Blanc, L. Villard, S. Daniel for the TropiSAR campaign, N. Bagdhadi and C. Lelong for the ENVIRO campaign as well as the ONERA ENVIRO team who contributed to the in-situ data acquisition for the optical/radar campaign. We also express our gratitude to Rolf Sheiber from DLR for providing the necessary trajectory files for BIOSAR E-SAR acquisition.

References

- Angelliaume, S.; Durand, P., Souyris, J.C., 2011. Ship detection using X-band dual-pol SAR data. In : IEEE International Geoscience and Remote Sensing Symposium (IGARSS). IEEE, Vancouver, Canada, 24-29 July 2011, pp.3827-3830.
- Arnaubec, A., Dubois-Fernandez, P., 2012. Analysis of PolInSAR precision for Forest and Ground Parameter Estimation in Tropical Context. In : IEEE International Geoscience and Remote Sensing Symposium (IGARSS). IEEE, Munich, Germany, 22-27 July 2012.
- Baque, R., Bonin, G., Ruault du Plessis, O., 2009. The airborne SAR-system: SETHI airborne microwave remote sensing imaging system. In : International Radar Conference - Surveillance for a Safer World. IEEE, Bordeaux, France, 12-16 October 2009.
- Canadell, J., Le Quéré, C., Raupach, M., Field, C., Buitenhuis, E., Ciais, P., Conway, T., Gillett, N., Houghton, N., Marland, G., 2007. Contributions to accelerating atmospheric CO₂ growth from economic activity, carbon intensity, and efficiency of natural sinks. *Proceedings of the National Academy of Sciences of the USA* 104(47), 18866–18870.
- Cantalloube, H., Dubois-Fernandez, P., 2006. Airborne X-band SAR imaging with 10 cm resolution: technical challenge and preliminary results. *IEE Radar, Sonar and Navigation* 153(2), 163–176.
- Cantalloube, H., Fromentin-Denoziere, B., Nahum, C., 2010. Towards a Polarimetric SAR Processor for Airborne Sensor. *PIERS Online* 6(5), 465–469.
- Cloude, S.R., Papathanassiou, K., 2003. A three stage inversion process for polarimetric SAR interferometry. *IEE Radar, Sonar and Navigation* 150(3), 125–134.
- Dreuillet, P., Cantalloube, H., Colin, E., Dubois-Fernandez, P., Dupuis, X., Fromage, P., Garestier, F., Heuze, D., Oriot, H., Peron, J.L., Peyret, J., Bonin, G., du Plessis, O.R., Nouvel, J.F., Vaizan, B., 2006. The ONERA RAMSES SAR: latest significant results and future developments. In : IEEE Conference on Radar. IEEE, Verona, NY, USA, 24-27 April 2006.
- Dubois-Fernandez, P., Souyris, J.-C., Angelliaume, S., Garestier, F., 2008. The compact polarimetry alternative for spaceborne SAR at low frequency. *IEEE Transactions on Geosciences and Remote Sensing* 46(10), 3208–3222.
- Dubois-Fernandez, P., Le Toan, T., Daniel, S., Oriot, H., Chave, J., Blanc, L., Villard, L., Davidson, M., Petit, M., 2012. The TropiSAR Airborne Campaign in French Guiana: Objectives, Description, and Observed Temporal Behavior of the Backscatter Signal. *IEEE Transactions on Geosciences and Remote Sensing*, in press.

- Dupuis, X., Dubois-Fernandez, P., Ulander, L., Gustavsson, A., 2012. 3 Year Temporal-Baseline Coherence at P Band. In: European Conference on Synthetic Aperture Radar (EU-SAR). Nuremberg, Germany, 23-26 April 2012.
- European Space Agency, 2008. BIOMASS Report for Assessment. ESA SP 1313/2.
- European Space Agency, 2012. BIOMASS Report for Selection, in press.
- Farr, T., 2001. Imaging radar in the Mojave desert ? Death Valley region. In: Workshop on the Martian highlands and Mojave desert analogs. Las Vegas, NV, USA, 20-27 October 2001.
- F-SAR. http://www.dlr.de/hr/en/desktopdefault.aspx/tabid-2326/3776_read-5691/.
- Garestier, F., Dubois-Fernandez, P., Champion, I. Forest Height Inversion Using High Resolution P-Band Pol-InSAR Data. IEEE Transactions on Geoscience and Remote Sensing 46(11), 3544–3559.
- Hajnsek, I., Kugler, F., Lee, S.-K., Papathanassiou, K.P., 2009. Tropical-Forest-Parameter Estimation by means of Pol-InSAR: The INDREX II Campaign. IEEE Transactions on Geoscience and Remote Sensing 47(2), 481–493.
- Hajnsek, I., Scheiber, R., Ulander, L., Gustavsson, A., Sandberg, G., Tebaldini, S., Guarnieri, A.M., Rocca, F., Bombardini, F., Pardini, M., 2008. BioSAR 2007. Technical assistance for the development of airborne SAR and geophysical measurements during the BioSAR 2007 experiment: Final report without synthesis, European Space Agency, ESA contract no. 20755/07/NL/CB.
- Hoekman, D.H., Verekamp, C., 2001. Observation of tropical rain forest trees by airborne high-resolution interferometric radar. IEEE Transactions on Geoscience and Remote Sensing 39(3), 584–594.
- Horn, R., 1996. The DLR airborne SAR project E-SAR, Geoscience and Remote Sensing Symposium, 1996. In : IEEE International Geoscience and Remote Sensing Symposium (IGARSS). IEEE, Lincoln, NE, USA, 27-31 May 1996, pp.1624-1628.
- Le Toan, T., Beaudoin, A., Riou, J., Guyon, D., 1992. Relating forest biomass to SAR data. IEEE Transactions on Geoscience and Remote Sensing 30(2), 403–411.
- Le Toan, T., Quegan, S., Davidson, M., Baltzer, H., Paillou, P., Papathanassiou, K., Plummer, S., Rocca, F., Saatchi, S., Shugart, H., 2011. The BIOMASS mission: Mapping global forest biomass to better understand the terrestrial carbon cycle, Remote Sensing of Environment 115(11), 2850–2860.
- McCauley, J.F., Schaber, G.G., Breed, C.S., Grolier, M.J., Haynes, C.V., Issawi, B., Elachi, C., Blom, R., 1982. Sub-surface valleys and geoarchaeology of the Eastern Sahara revealed by Shuttle Radar. Science 218, 1004–1020.
- Neumann, M., Ferro-Famil, L., Reigber, A., 2010. Estimation of Forest Structure, Ground, and Canopy Layer Characteristics From Multibaseline Polarimetric Interferometric SAR Data. IEEE Transactions on Geoscience and Remote Sensing 48(3), 1086–1104.
- Paillou, P., Dreuillet, P., 2002. The PYLA?01 experiment: Flying the new RAMSES P-band facility. In: Workshop AIR-SAR Earth Science and Application, Pasadena, CA, USA, 4-6 March 2002.
- Paillou, P., Lopez, S., Farr, T., Rosenqvist, A., 2010. Mapping Subsurface Geology in Sahara Using L-Band SAR: First Results From the ALOS/PALSAR Imaging Radar. IEEE Journal of Selected Topics in Applied Earth Observations and Remote Sensing 3(4), 632–636.
- Paillou, P., Ruault du Plessis, O., Coulombeix, C., Dubois-Fernandez, P., Bacha, S., Sayah, N., Ezzine, A., 2011. The TUNISAR experiment: Flying an airborne P-Band SAR over Southern Tunisia to map subsurface geology and soil salinity. In: PIERS. Marrakesh, Morocco, 20-23 March 2011.
- Richard, J., Enjolras, V., Schoeser, C., Angelliaume, S., Durand, P., 2010. An innovative spaceborne radar concept for global maritime surveillance: Description and performance demonstration. In: IEEE International Geoscience and Remote Sensing Symposium (IGARSS). IEEE, Honolulu, HI, USA, 25-30 July 2010, pp.257-259.
- Rignot, E., Zimmermann, R., van Zyl, J., 1995. Spaceborne applications of P band imaging radars for measuring forest biomass. IEEE Transactions on Geoscience and Remote Sensing 33(5), 1162–1169.
- Rosen, P.A., Hensley, S., Wheeler, K., Sadowy, G., Miller, T., Shaffer, S., Muellerschoen, R., Jones, C., Zebker, H., Madsen, S., 2006. UAVSAR: a new NASA airborne SAR system for science and technology research. In: IEEE Conference on Radar. IEEE, Verona, NY, USA, 24-27 April 2006.
- Saatchi, S., Halligan, K., Despain, D.G., Crabtree, R.L., 2007. Estimation of Forest Fuel Load From Radar Remote Sensing. IEEE Transactions on Geoscience and Remote Sensing 45(6), 1726–1740.
- Sandberg, G., Ulander, L.M.H., Fransson, J.E.S., Holmgren, J., Le Toan, T., 2011. L- and P-band backscatter intensity for biomass retrieval in hemiboreal forest. Remote Sensing of Environment 115(11), 2874–2886.
- Sarabandi, K., Ulaby, F.T., Tassoudji M.A., 1990. Calibration of polarimetric radar system with good polarisation isolation. IEEE Transactions on Geoscience and Remote Sensing 28(1), 70–75.
- Ulander, L.M.H., Gustavsson, A., Dubois-Fernandez, P., Dupuis, X., Fransson, J.E.S., Holmgren, J., Wallerman, J., Eriksson, L., Sandberg, G., Soja, M., 2011. BIOSAR 2010 - A SAR campaign in support to the BIOMASS mission. In: IEEE International Geoscience and Remote Sensing Symposium (IGARSS). IEEE, Vancouver, Canada, 24-29 July 2011, pp.1528–1531.